A STRATEGY FOR INVESTIGATING AND MODELING INTERNAL WAVE SOURCES AND SINKS

Eric A. D'Asaro

Applied Physics Laboratory, College of Ocean and Fishery Sciences, University of Washington, Seattle, WA 98105-6698

ABSTRACT

We do not know what forces the internal wave field, except in the broadest terms. The spectral levels are remarkably uniform, but the likely sources have obvious spatial and temporal variability. This argues that long-range horizontal propagation of energy must be an important factor in "smoothing out" the irregularity of the sources. Research suggests that only low-mode, low-frequency internal waves are capable of propagating significant distances. In the short term, measurements of the directional spectra of these waves should therefore reveal the dominant energy sources for the internal wave field. In the longer term, a global model of the internal wave field and its associated diapycnal mixing could be constructed by simulating the generation, propagation, and dissipation of these low-mode, low-frequency waves. This is a worthy long-term goal for internal wave research.

WHAT DO WE WANT TO KNOW?

In the last 20 years we have learned a great deal about the spectral and spatial distribution of internal wave energy. Measurements show the spectrum is remarkably stable compared, for example, with that of surface waves. It is therefore useful to talk about a "universal" spectral shape for internal waves (Garrett and Munk, 1979). A nearly universal spectrum is consistent with theory (Müller et al., 1986), which predicts that wave–wave interactions produce an internal wave spectrum that is not very sensitive to the details of the wave sources. More recently, direct comparisons between measurements of the kinetic energy dissipation rate, ϵ, and values predicted by wave–wave interaction theories (see Gregg and Padman discussions, this volume) show some agreement, although the story is far from complete at present. Notably, although only small variations are seen in the *spectral level*, they correspond to much larger variations in ϵ, a *spectral transfer rate*. The internal wave field thus looks much more dynamic and much less universal when viewed in terms of rates rather than levels.

In contrast, only modest progress has been made in determining the sources of the internal wave field. There are variations in the energy and spectral level (Wunsch and Webb, 1979; Levine et al., 1985). Some investigators[1] have found correlations between sources and internal wave characteristics. Levine et al. (1985) find a wind forced signal in the Arctic Ocean; Padman and Dillon (1991) and Levine et al. (1983) find tidally forced signals; Kunze and Sanford (1984) find strong signals associated with mesoscale rings and fronts; and D'Asaro (1985a) finds a signal from strong storms. In general, however, it has been difficult to find any clear association between the wave field's sources and sinks and its behavior. This is not due to any lack of

[1]This is clearly an incomplete list. I apologize to investigators who have not been mentioned.

potential sources and sinks. Idealized calculations indicate that wind stress (D'Asaro, 1985b), surface waves (Watson, this volume), bottom topography (Bell, 1975), and geostrophic currents (Watson, 1985), among others, could all potentially be important. The problem is distinguishing among these sources.

I propose that the next goal of internal wave research should be to find and quantify the internal wave sources. The key to the strategy is to realize that only low-mode, low-frequency internal waves can propagate substantial distances (>1000 km) in the ocean. These waves must therefore supply energy to the wave field in regions where the sources are weak. Measurements of the directional spectrum of these low-mode waves should reveal their sources, since different sources will undoubtedly be distributed differently in space and time. In the long term, we might consider working toward global models of the internal wave field which track energy from sources into propagating low modes, back into the local wave field, and finally to local dissipation and diapycnal mixing. The remainder of this paper will elaborate on these ideas.

THEORETICAL RESULTS

Scales

Internal waves span a wide range of scales and thus a wide range of dynamical regimes. Figure 1 shows the spectral domain of internal waves as a function of WKB normalized, hydrostatic, vertical wavenumber (horizontal axis), frequency (vertical axis), and horizontal

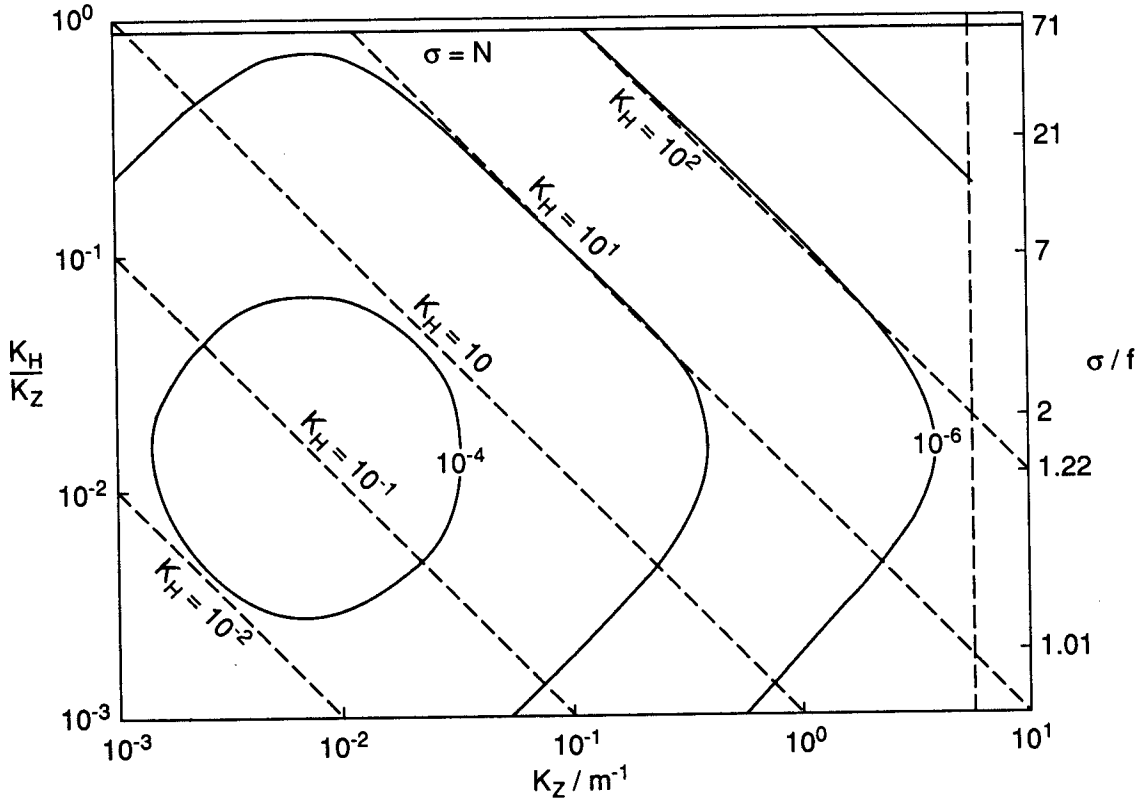

Fig. 1. Spectral density of internal wave energy according to GM76 [after McComas, 1977] as a function of vertical wavenumber K_Z (horizontal axis), frequency σ (vertical axis), and horizontal wavenumber K_H (dashed diagonal lines) using the hydrostatic approximation.

wavenumber (diagonal lines). The distribution of energy is contoured (Garrett and Munk, 1975). Most of the energy is at low wavenumbers and low frequencies.

Propagation

Internal waves can propagate horizontally and thus spread energy away from source regions. The horizontal group speed is contoured in Fig. 2 (dashed curves). Only the low modes have significant speeds.

Very nearly inertial, low-mode waves cannot exist, since the β effect changes f by more than $\sigma - f$ over their inverse horizontal wavenumber (Fu, 1981). This region is indicated by the shaded region in the lower left-hand corner of Fig. 2. Vorticity gradients in geostrophic flows are usually comparable to β and sometimes far exceed it (Kunze, 1985). The propagation of internal waves will be strongly modified by interactions with these flows. The region of limited propagation will thus be considerably larger than the "no waves" region in Fig. 2.

The low phase speed of many internal waves limits their propagation. The frequency of waves propagating in a background flow will be Doppler shifted by an amount $\Delta\sigma = \vec{k}\cdot\vec{U}$, where $\vec{k}$ is their horizontal wavenumber and $\vec{U}$ is the change in the background velocity through which they have propagated. If $\Delta\sigma$ exceeds $\sigma - f$, the waves may be Doppler shifted into a critical

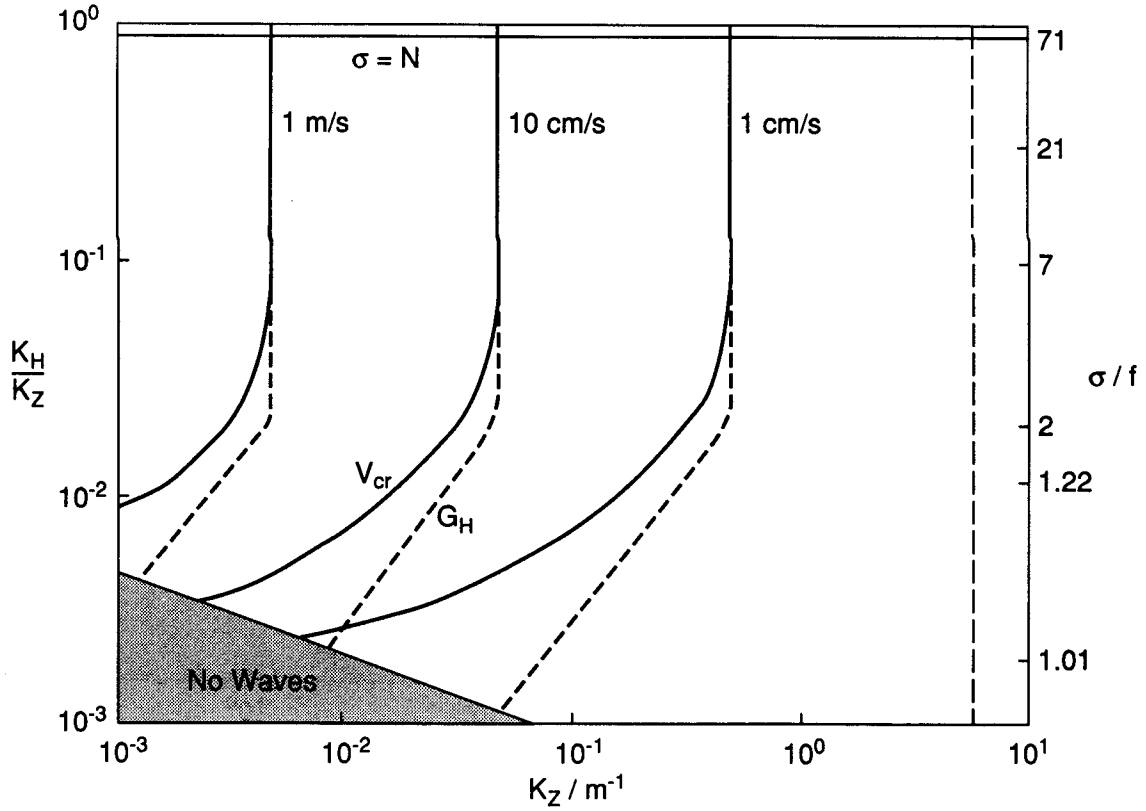

Fig. 2. Contours of hydrostatic, WKB horizontal group speed G_H (dashed curves) and U_{cr}, the background velocity necessary for critical layers (solid curves). The region of waves excluded by the β effect is shaded.

layer. Even if they are not, they will be strongly distorted. Contours of the background velocity necessary for the formation of critical layers are plotted in Fig. 2; $U_{cr} = (\sigma - f)/|\vec{k}|$. Because the internal wave field itself commonly has velocities approaching 10 cm/s, waves with $U_{cr} <$ 10 cm/s are unlikely to propagate far. This defines a region of strong wave–wave interaction at mid and high wavenumbers in which wave propagation is limited. Mesoscale geostrophic motions commonly have velocities of 10–100 cm/s. Waves with $U_{cr} < 100$ cm/s will not propagate far in regions with such a mesoscale eddy field. Oceanic velocities in excess of 100 cm/s are uncommon except in the strongest currents. The propagation of waves with $U_{cr} > 100$ cm/s will usually not be inhibited by interaction with ocean currents.

Wave–Wave Interaction

The sources of internal waves are believed to be concentrated at low wavenumbers. Wave–wave interaction theories predict a cascade of energy from small to large wavenumbers, as indicated by the arrows in Fig. 3. Although there is some disagreement (in details) between the results of resonant and eikonal approximations (Müller et al., 1986), there is consensus that these interactions feed energy to small-scale dissipation and mixing. The transfer of energy

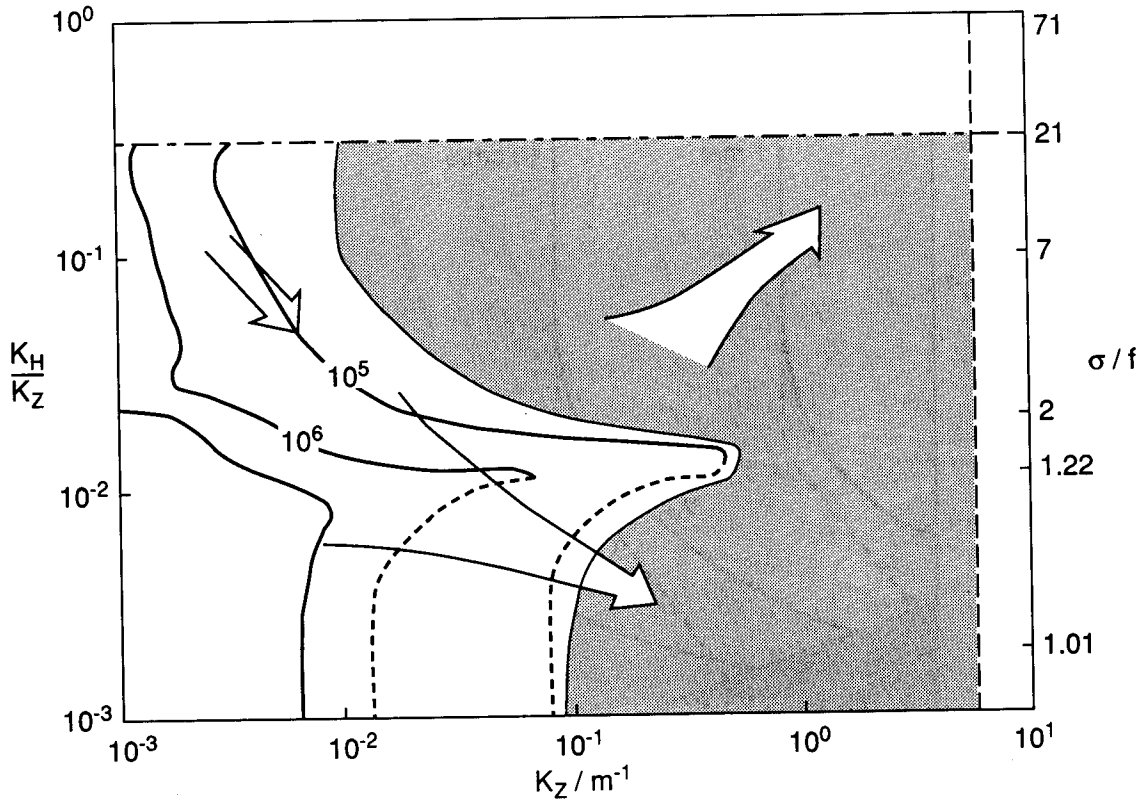

Fig. 3. Decay time for a 10% spike in the spectrum shown in Fig. 1 [from McComas, 1977]. The region where this time is shorter than a wave period is shaded. Dashed contours indicate that spike grows. Arrows indicate direction of energy flux due to nonlinear interactions: resonant theory [McComas, 1977] outside of shaded region, and eikonal [Henyey et al., 1986] inside.

between waves of different scales is due to the nonlinearity of the equations of motion, and thus becomes stronger at higher wavenumbers. If the rates are high enough, the waves interact so fast that they can no longer be described as freely propagating. Estimates of the energy transfer rates (Fig. 3) indicate that this limit is reached for waves with wavenumbers greater than 10–100 m^{-1}, as indicated by the shading. At wavenumbers smaller than this, waves can propagate for some time before they lose their energy to the rest of the wave field. Contours of this interaction time (Fig. 3) show a strong dependence on vertical wavenumber. Only the small wavenumbers (i.e., the low modes) have interaction times longer than 10 days (10^6 s).

Which Waves Can Propagate?

A "mean free path" L_{free} for horizontally propagating internal waves is estimated as the product of the interaction time τ_{iw} multiplied by the horizontal group velocity G_H. Approximate contours of L_{free} = 1000 km are shown in Fig. 4. Only a relatively small range of waves can propagate 1000 km. Another, perhaps more accurate estimate of L_{free} is given in E. Hirst's paper in this volume.

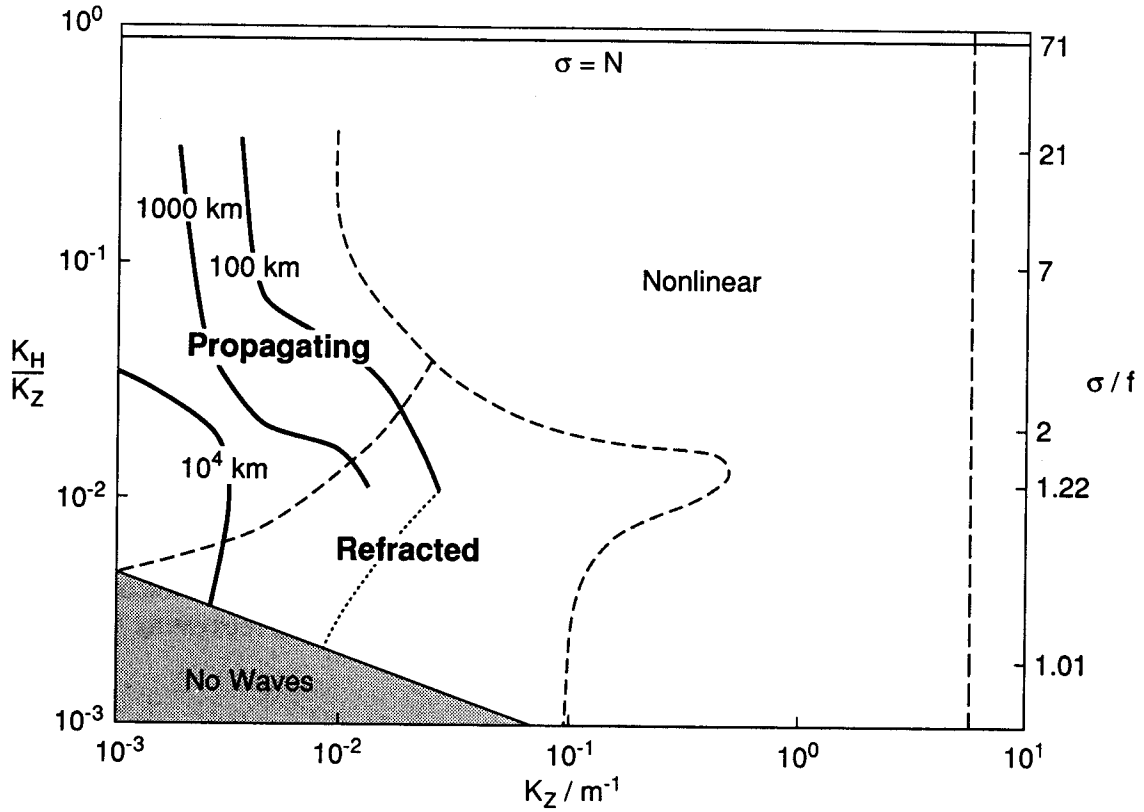

Fig. 4. Spectral location of Propagating Waves. High-wavenumber and high-frequency waves (Nonlinear) interact strongly and cannot propagate far. Many near-inertial waves (Refracted) are strongly refracted by internal waves and geostrophic currents and also cannot propagate far. The edge of this domain (dashed curve) is defined by U_{cr} = 0.2 m/s. Inertial, low-mode waves are prohibited by the β effect (No Waves). Propagation distance of low-mode, somewhat superinertial waves (Propagating), computed by hand from Figs. 2 and 3, is contoured. The end of the contours indicates inability to interpolate the figures. Dotted contour indicates that perturbations grow.

Figure 4 partitions the internal wave domain into various dynamical regions based on the above considerations. At high wavenumbers, τ_{iw} is short, and the waves are strongly nonlinear. They cannot propagate far. At lower wavenumbers, the waves become increasingly linear but still have small values of L_{free}. At low wavenumbers, but very close to the inertial frequency, wave propagation is limited by the β effect and interaction with the mesoscale flow. Only low modes with frequencies somewhat above f can propagate basinwide. I will call these "Propagating Waves."

THE ROLE OF PROPAGATING WAVES

Now consider a region of the ocean far from strong sources of internal waves such as wind, bottom topography, and internal tides generated on the shelves. Pick a region in the middle of a large ocean, over flat topography. The IWEX site might not be a bad choice! The chances are that the local sources are well below average. Nevertheless, the internal wave field is comparable to that found at more energetic sites. Wave interaction calculations and typical dissipation rates suggest that this wave field should lose most of its energy in 50–100 days, yet there is little evidence that this happens. Where does the energy come from to renew the wave field in this region? I suggest that it is supplied by the low-mode, large L_{free}, Propagating Waves discussed above. [2]

If, as indicated in Fig. 3, the major sources of internal waves are at low modes and low frequencies, much of their energy will be put into the Propagating Waves. These waves will disperse from the region where they were generated, releasing energy only slowly and over a wide region. Consequently, the Propagating Waves will flux energy away from the source regions. In a sink region, therefore, the directional spectrum of Propagating Waves will point toward the sources, much as surface-wave swell spectra point toward distant storms. Measurement of this spectrum should teach us about the distribution of sources.

Another consequence is that away from strong local sources the properties of the local internal wave field are determined by the rate at which the Propagating Waves give up energy. This rate is slow because these waves are nearly linear; thus resonant wave–wave interaction theory should be accurate. Other interactions such as scattering from topographic features may also be important. The local rate of energy loss from the Propagating Waves should equal, on average, the local rate of energy dissipation and thus govern the local rate of internal wave mixing. We should therefore observe a relationship between the field of Propagating Waves, the local internal wave spectrum, and the dissipation rate.

EVIDENCE FOR PROPAGATING WAVES

Existing evidence, although limited, supports these ideas.[3] During IWEX (Müller et al., 1978), detailed measurements were made of the internal wave field in the Sargasso Sea (27°N, 70°W), a region probably weak in local sources. During the limited time of the measurements (42 days), waves with frequencies between f and about $4f$ were significantly anisotropic, whereas those at higher frequencies were nearly isotropic. The anisotropic waves were all propagating toward the southeast, i.e., away from the North American continental shelf. Semidiurnal tidal energy, both anisotropic and dominated by low modes, looks like a Propagating Wave generated on the shelf. Interestingly, Müller et al. (1978) were so unconcerned with sources that the season of the measurements is not even mentioned!

Evidence for propagation of internal waves over long distances is provided by Fu's (1981) analysis of long-term abyssal moorings in the North Atlantic. The large-scale internal wave field was modeled by linearly propagating a Garrett-Munk-like wave field with no inertial peak northward from the equator. The model (Fig. 5) produces both near-inertial peaks and superinertial spectra which agree remarkably well with the abyssal data (given the simplicity of the model). This supports the idea that internal waves can propagate significant distances. The data are insufficient to determine the wavenumbers of the waves that propagate. The model worked poorly in the upper ocean, in the thermocline, and over rough topography. Fu (1981) models these features, with some success, as due to local sources of near-inertial waves.

Lai and Sanford (1986) observed the local generation of low modes after the passage of a hurricane near the New England continental slope. First the lowest mode was observed and then higher modes; the timing was consistent with generation at a site 80 km away.

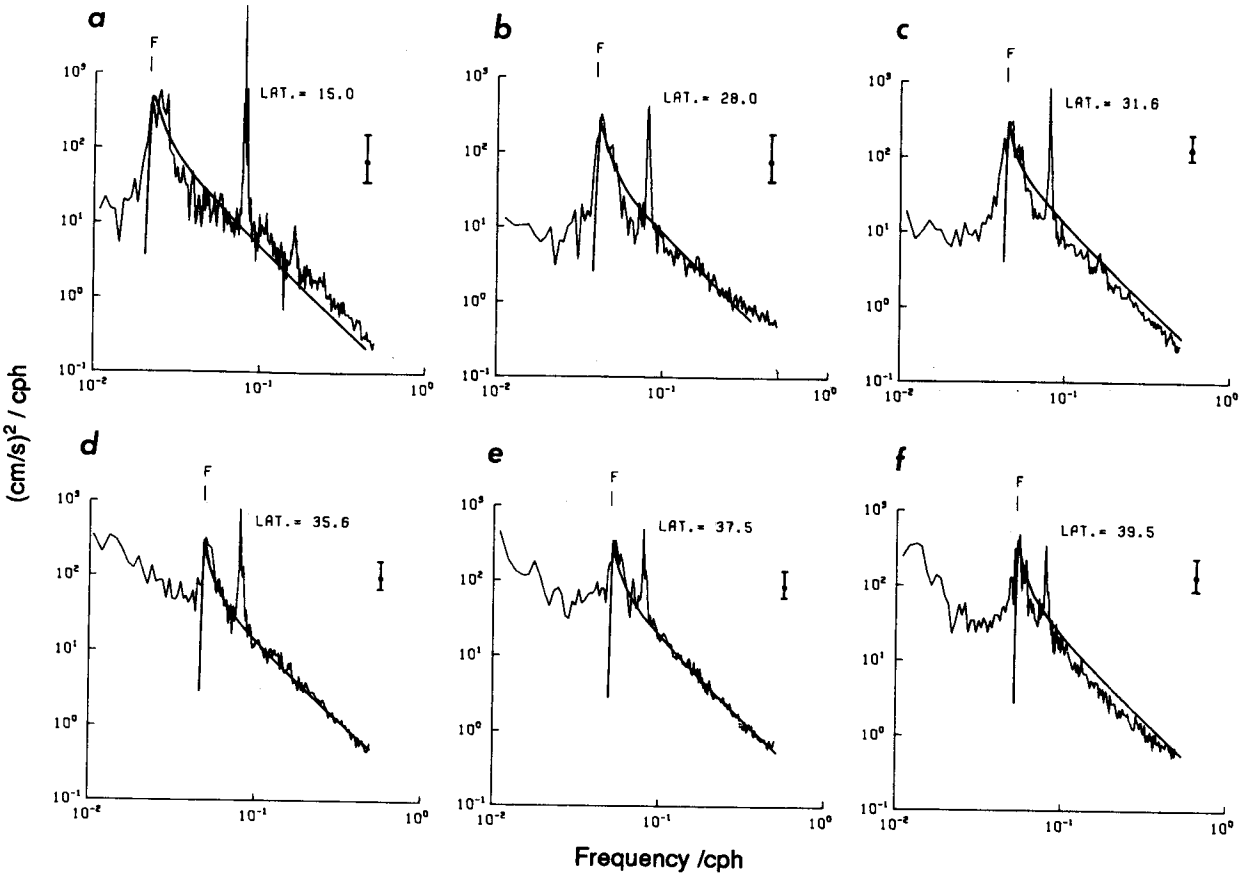

Fig. 5. Model (smooth curves) and observed spectra of horizontal kinetic energy at 4000 m measured during long-term moorings in the North Atlantic. Inertial frequency and latitude are marked. [from Fu, 1981]

[2] I believe this idea originates with the unpublished Johnson and Cox manuscript.

[3] Perhaps my knowledge, rather than the evidence, is limited.

WIND FORCING

We do not know which of the possible sources of internal wave energy is most important. Rather than attempting to understand them all, we might look at just one and ask whether the data are consistent with its being the primary source. I propose that wind forcing is a primary candidate, although tidal forcing is another possibility. Internal waves in the thermocline usually show a dominance of downward propagating, near-inertial energy. Examples include data taken by Leaman and Sanford (1975), D'Asaro (1984), and Müller et al. (1978). Atmospheric forcing is the obvious source of this asymmetry.

Mixed Layer Inertial Currents

Perhaps the best understood source of internal waves is excitation of mixed-layer inertial motions by the wind. Because atmospheric wind fluctuations are typically both much larger than a Rossby radius in the ocean and move faster than the lowest baroclinic phase speed, the wind stress tends to excite mostly near-inertial waves (Gill, 1984). It has been apparent since the first near-surface current meter records that strong mixed-layer inertial currents are generated by fluctuating wind stresses (Webster, 1968). A simple slab mixed-layer model does a decent job of simulating this process under most conditions, as was first demonstrated by Pollard and Millard (1970). Mixed-layer inertial currents and the energy transferred from the wind to these currents can be estimated from wind data using this model.

How well can we predict the flux of energy from the wind to mixed-layer inertial currents? An example of such a calculation using real wind measurements is shown in Fig. 6. The required

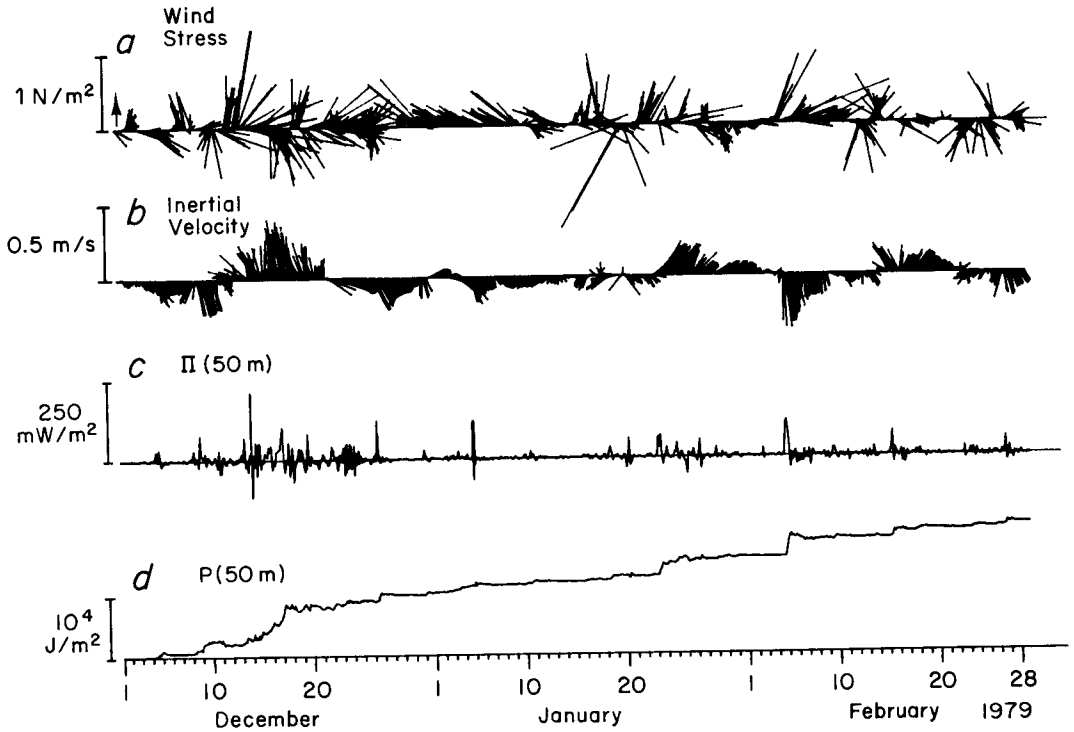

Fig. 6. Inertial-energy flux computed for NOAA Data Buoy Center buoy 46006 near 41°N, 140°W. (a) Wind stress computed with Garratt (1977) drag law. (b) Mixed-layer inertial velocity computed using 50 m mixed-layer depth. (c) Energy flux to mixed-layer inertial motions. (d) Integrated energy flux.

data are the wind stress (top panel), a drag law, and the mixed layer depth, here assumed to be 50 m. The resulting energy flux (bottom two panels) is highly intermittent and is dominated by a few storms. For 10 years of data from Ocean Weather Station P, for example, the kurtosis of the energy flux was estimated at 360 and the average November energy flux was increased 60% by a single storm (D'Asaro, 1985b). Storms are clearly important, and wind stress data are required at least every few hours. Operational weather products probably do not give these winds with sufficient accuracy over the ocean, (Thomson, 1983). Furthermore, the drag coefficient can vary by a factor of 2 during storms (Geernaert, 1988), resulting in significant changes in the computed inertial currents (D'Asaro, 1985a). Because of these factors, accurate predictions of mixed-layer inertial currents can probably not be made using operational weather products until predictions of winds over the ocean are significantly improved.

Figure 7 shows the 10 year average annual cycle of energy flux to mixed-layer inertial currents computed using a simple slab model and climatological mixed-layer depth (D'Asaro, 1985b). The flux is large in the fall and winter and small in the summer because of the stronger wind in the winter. It is largest in the early fall because of the thinner mixed layers. Although the proper calculations have not been made, the large-scale spatial pattern is probably quite similar to that of the wind stress (Fig. 8). The important point is that clear seasonal and large-scale geographical signals exist. We do not know how well operational products can predict these signals, although prediction of seasonal and regional averages is likely to be more accurate than that of local statistics.

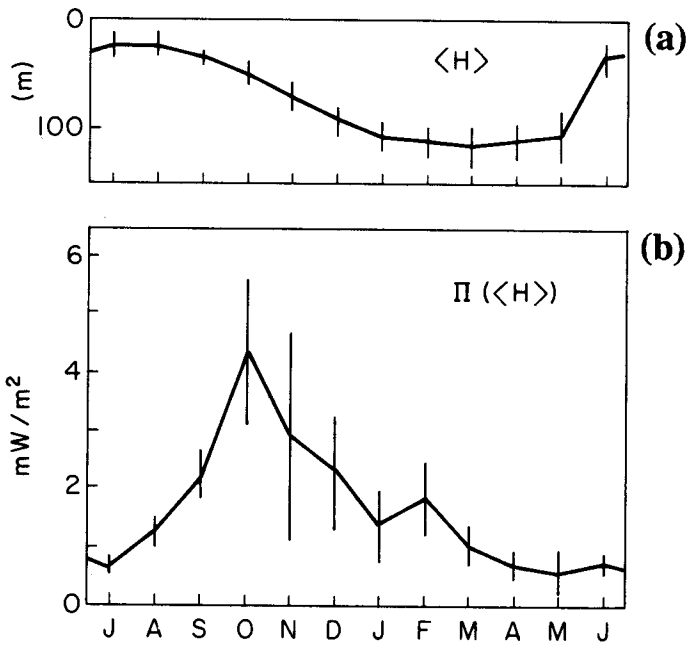

Fig. 7. Annual cycle of inertial energy flux at OWS-P (50°N, 145°W). (a) Annual cycle of mixed-layer depth. (b) Annual cycle of energy flux to mixed-layer inertial currents computed as in Fig. 6 but using mixed-layer depth from (a).

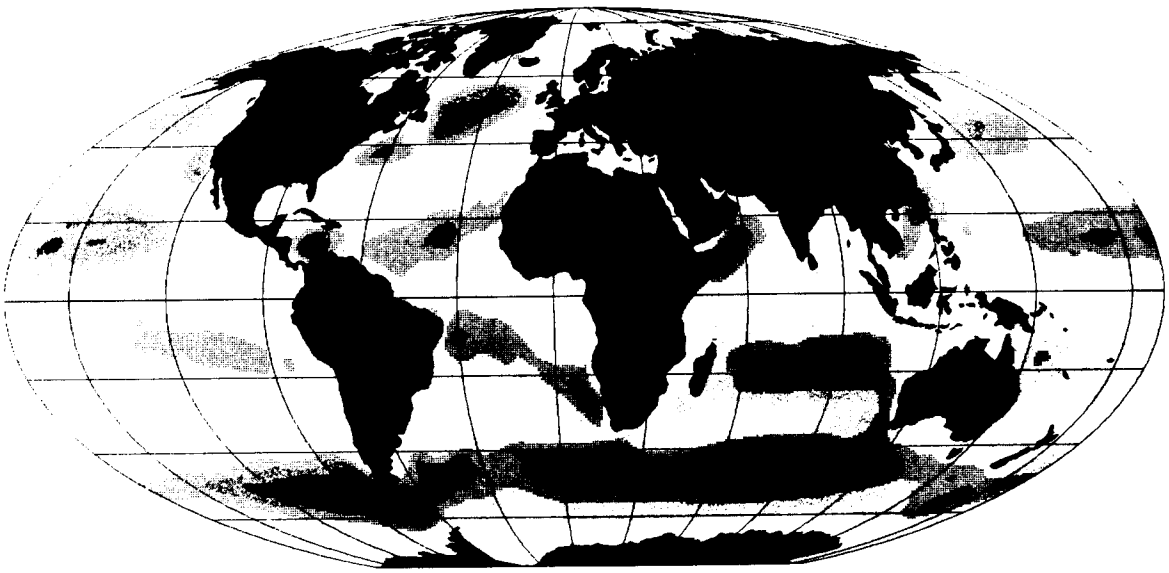

Fig. 8. Annual wind stress magnitude (Hellerman and Rosenstein, 1983). Contour level is 0.1 Pa. [from Briscoe, 1984]

Low-Mode, Near-Inertial Waves

Most of the energy in mixed-layer inertial currents probably propagates into the stratified ocean in the form of local and propagating near-inertial internal waves. Figures 9–12 show a simulation of the ocean's response to a single storm. The forcing, latitude, and stratification are tuned to match the conditions observed during early October 1987 as part of the OCEAN STORMS experiment. The model is a two-dimensional variant of Price's (1983) hurricane model, with 21 layers, full nonlinearity, hydrostatic dynamics, a β plane, and a vertical viscosity of 2×10^{-4} m^2/s, which improves its fit with the data. It is forced in the mixed layer by a Gaussian storm centered at $y = 0$ (47.5°N).

The response of the model ocean to this storm is almost entirely near-inertial. Figure 9 shows depth-time contours of the inertial amplitude as a function of depth and time in the upper kilometer. The model storm forces mixed-layer inertial currents of about 40 cm/s. For the first 10 days after the storm, the inertial energy stays in the mixed layer while the β effect increases the north-south wavenumber of the currents as described by D'Asaro (1989). There is some slight penetration of energy into the thermocline owing to the imposed vertical viscosity. Eventually, the horizontal wavenumber becomes large enough for linear wave propagation to occur. Between days 300 and 320, almost all the mixed layer energy is transferred to the upper thermocline and to low-mode, near-inertial waves. Contours of inertial speed in the latitude-time plane (Figs. 10–12) show the distinct separation and propagation of modes 1 (starting on day 306) and 2 (starting on day 320). Both modes are seen at the surface (Fig. 10) and in the upper thermocline (Fig. 11), but only mode 2 is seen at 1000 m (Fig. 12) because this is near the zero crossing of mode 1. Similar results were seen in simulations by Gill (1984).

The low modes rapidly propagate southward away from the source region. In the simulation, waves in the thermocline 2000 km south of the storm have speeds of about 1 cm/s and verti-

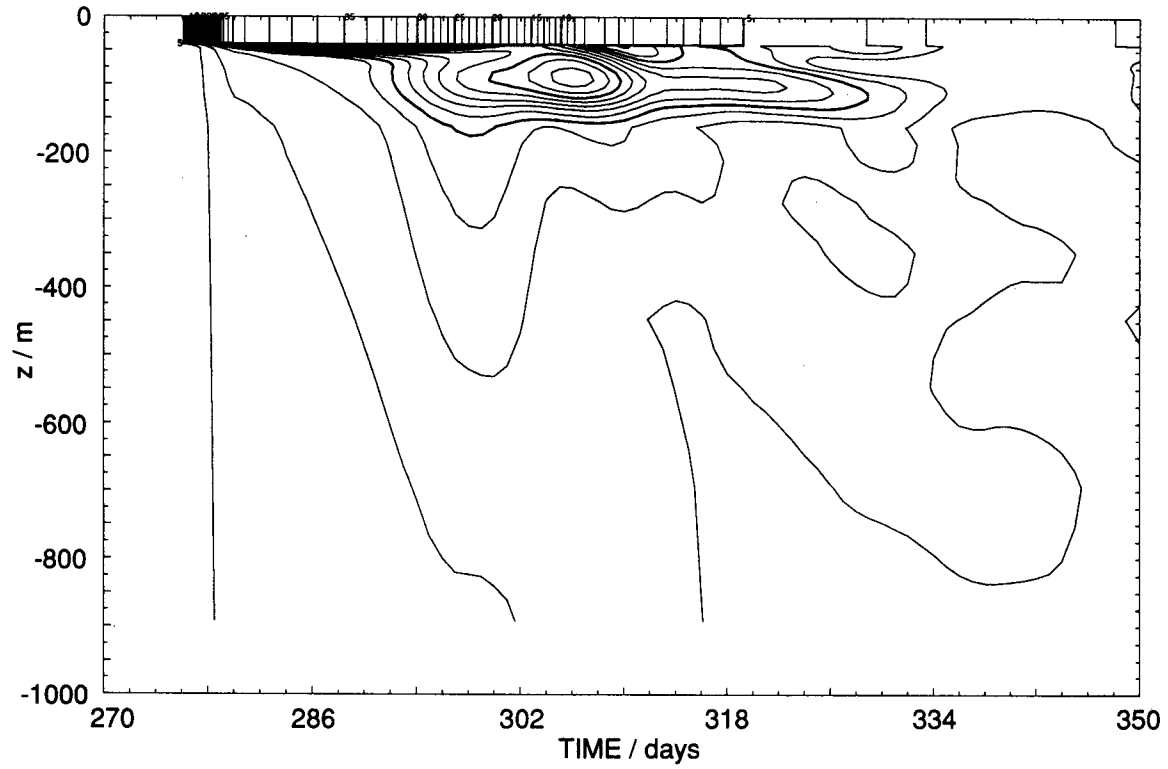

Fig. 9. Inertial speed as a function of depth and time directly beneath the storm ($y = 0$) for simulation of ocean response to a strong storm. Contour interval is 1 cm/s.

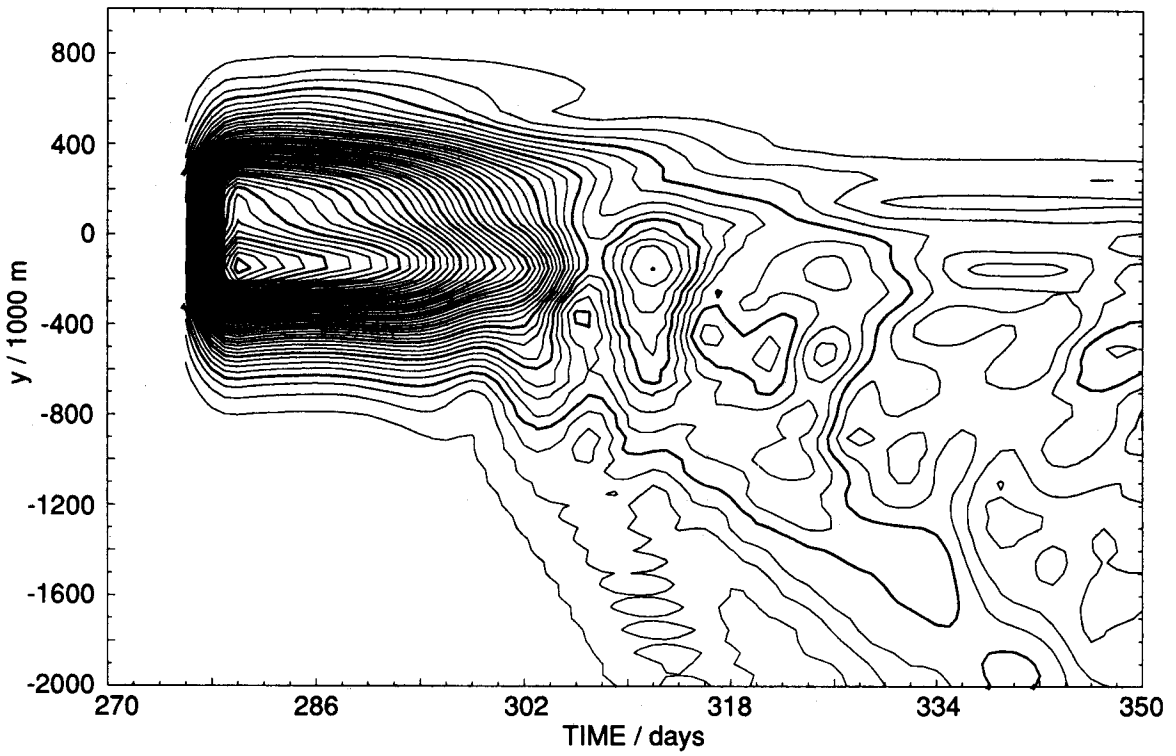

Fig. 10. Inertial speed at the surface as a function of meridional distance and time. Location and size of storm are clearly seen as is propagation of energy to the south. Contour interval is 1 cm/s.

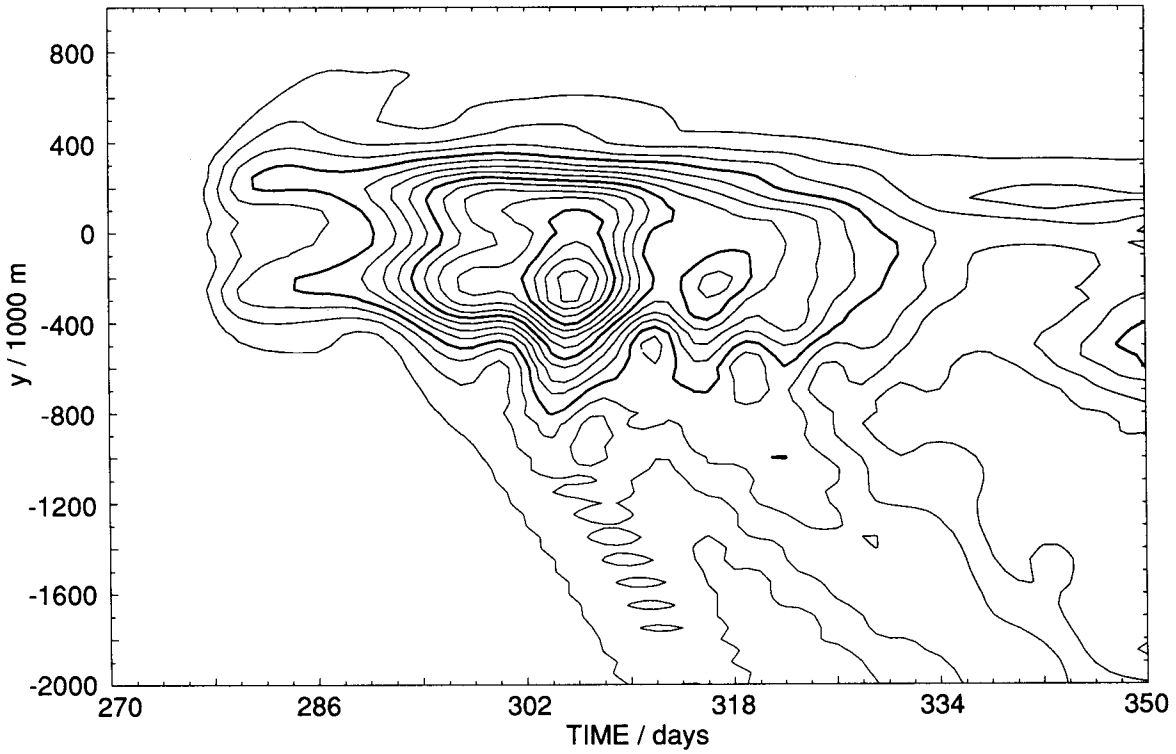

Fig. 11. Inertial speed at 100 m as a function of meridional distance and time. Comparison with Fig. 10 shows propagation of energy from the mixed layer starting near day 286 and southward propagating modes. Contour interval is 1 cm/s.

cal displacements of about 1 m for at least 20 days. These waves have distinct properties. They are low mode and have a meridional wavelength near 100 km. Their frequency is about $\beta\Delta y$, where Δy is the meridional distance from the storm, which equals $1.3f$ near 30°N. A fully three-dimensional calculation would show a zonal wavelength near U/f, where U is the advection speed of the storm. Although wave–wave interactions are not included in the model, these scales are clearly in the range of the "Propagating Waves" shown in Fig. 4. These waves should therefore not be strongly attenuated by interaction with the rest of the wave field. Their signatures are distinct and should be easily measured, given the proper instrumentation

In this simulation, the energy put into the inertial currents, averaged over the 30 day length of the ocean response, is about 10^{-3} W/m^2. The average wintertime fluxes estimated in Fig. 7 are several times this. Furthermore, because the propagating waves always go equatorward, the total southward flux is the result of all forcing north of a given location. It would not be unreasonable, therefore, to expect the peak wintertime amplitude of Propagating Waves to be several times that shown in Figs. 9–12. A far weaker signal should be expected in the summer.

SOME SUGGESTIONS FOR RESEARCH

How can we detect Propagating Waves generated by storms? The signal is so weak that the waves from a single storm will probably not be obvious unless the storm is very strong (e.g., Lai and Sanford, 1986). Measurements will therefore have to be designed to detect the signal. The key appears to be averaging either in the vertical, to isolate the low-mode structure, or in the

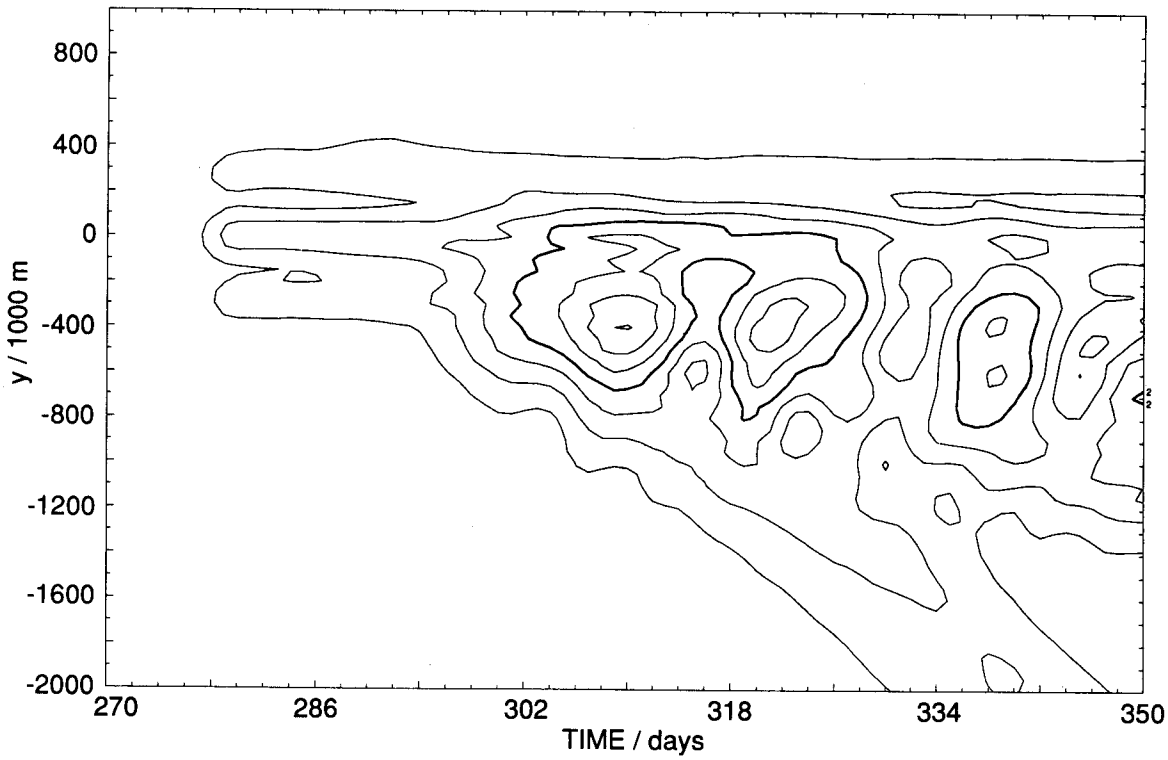

Fig. 12. Inertial speed at 1000 m as a function of meridional distance and time. Contour interval is 0.5 cm/s.

horizontal, to isolate the large horizontal scales, as well as filtering in time to isolate the distinct frequency. One approach would be to use integrating temperature sensors to filter out the high modes. Vertical or horizontal acoustic propagation is another promising technique. Given the strong seasonal cycle expected of wind forcing, a long time series of directional measurements of the low-mode waves seems like the most promising sampling scheme. A subtropical location south of the wintertime generation region that is subject to Propagating Waves generated by late summer hurricanes and a large internal tide source would seem ideal.

We also need better theoretical descriptions of the processes controlling propagation of low modes. Can we really expect to see these low mode signals? This depends on how energy gets out of them. Calculations of resonant wave–wave interaction, which should be accurate for these weakly nonlinear waves, should be reexamined to include the effects of directionality, depth, and path-varying stratification. Topographic features and mesoscale eddies may scatter energy from these propagating waves into the local internal wave field. We don't know how to estimate these effects at present.

TOWARD A GLOBAL MODEL OF THE INTERNAL WAVE FIELD

Some oceanographers consider small-scale processes a source of noise and a sink for money. But they still look to the small-scale research community for estimates of the magnitude and variability of small-scale heat, salt, and momentum transport. Although we have little to offer for momentum transport, I believe we can envision how a predictive model of diapycnal mixing due to internal waves could be constructed.

First, we need to quantify at least some of the sources of internal waves. The time and space variability of the sources is a key factor because it will allow us to distinguish various sources in data. As mentioned previously, I think we have a good start in quantifying the generation by wind. Tidal generation should also be investigated. Initially, it is probably not necessary to quantify all the possible sources since it will eventually become apparent if we are missing a major one. It certainly would be enlightening, for example, to see what an internal wave field generated only by the wind would look like!

Second, we need to understand how the energy from these sources is distributed between the local wave field and the Propagating Waves. For wind-generated energy in the absence of mesoscale eddies, we can probably estimate this. The effect of mesoscale motions is not well studied.

Third, we need to know how far the Propagating Waves travel and how they give up their energy. It seems likely, as argued here, that only a small range of low-mode waves can propagate significant distances. If true, this greatly simplifies the problem. There is ample room for both observation and theory here. Our ignorance appears to be due to inattention, not hard technical problems, so advances should be rapid.

Fourth, we need to know how the energy supplied to the local wave field by local sources and by the Propagating Waves cascades through the local wave field to mixing. Great progress is being made here, but we are not yet finished.

Acknowledgments

Thanks to Peter Müller, Mel Briscoe, Frank Henyey, and Terry Ewart for stimulating these ideas. The Winter Workshop provided a great excuse to work them out and write them down. This work was supported by ONR contract N00014-89-C-0111 and ONR grant N00014-90-J-1104.

REFERENCES

Bell, T. H., Jr., 1975: Topographically generated internal waves in the open ocean. *J. Geophys. Res.*, **80**, 320–327.

Briscoe, M. G., 1984: The monthly variability of upper-ocean internal wave energy: A progress report on the correspondence with wind stress. In *Internal Gravity Waves and Small-Scale Turbulence, Proceedings, Hawaiian Winter Workshop*, P. Müller and R. Pujalet, Eds., 129–150, Hawaii Institute of Geophysics, Honolulu.

D'Asaro, E. A., 1984: Wind forced internal waves in the North Pacific and Sargasso Sea. *J. Phys. Oceanogr.*, **14**, 781–794.

D'Asaro, E. A., 1985a: Upper ocean temperature structure, inertial currents, and Richardson numbers observed during strong meteorological forcing. *J. Phys. Oceanogr.*, **15**, 943–962.

D'Asaro, E. A., 1985b: The energy flux from the wind to near-inertial motions in the surface mixed layer. *J. Phys. Oceanogr.*, **15**, 1043–1059.

D'Asaro, E. A., 1989: The decay of wind-forced mixed layer inertial oscillations due to the β effect. *J. Geophys. Res.*, **94**, 2045–2056.

Fu, L.-L., 1981: Observations and models of inertial waves in the deep ocean. *Rev. Geophys.*, **19**, 141–170.

Garratt, J. R., 1977: Review of drag coefficients over oceans and continents. *Mon. Wea. Rev.*, **105**, 915–929.

Garrett, C. J. R., and W. H. Munk, 1975: Space-time scales of internal waves: A progress report. *J. Geophys Res.*, **80**, 291–297.

Garrett, C. J. R., and W. H. Munk, 1979: Internal waves in the ocean. *Ann. Rev. Fluid Mech.*, **11**, 339–369.

Geernaert, G. L., 1988: Measurements of the angle between the wind vector and wind stress vector in the surface layer over the North Sea. *J. Geophys. Res.*, **93**, 8215–8220.

Gill, A. E., 1984: On the behavior of internal waves in the wakes of storms. *J. Phys. Oceanogr.*, **14**, 1129–1151.

Hellerman, S., and M. Rosenstein, 1983: Normal monthly wind stress over the world ocean with error estimates. *J. Phys. Oceanogr.*, **13**, 1093–1104.

Henyey, F. S., J. Wright, and S. M. Flatté, 1986: Energy and action flow through the internal wave field: An eikonal approach. *J. Geophys. Res.*, **91**, 8487–8495.

Kunze, E., 1985: Near-inertial wave propagation in geostrophic shear. *J. Phys. Oceanogr.*, **15**, 544–565.

Kunze, E., and T. B. Sanford, 1984. Observations of near-inertial waves in a front. *J. Phys. Oceanogr.*, **14**, 566–581.

Lai, D. Y., and T. B. Sanford, 1986: Observations of hurricane-generated, near-inertial slope modes. *J. Phys. Oceanogr.*, **16**, 657–666.

Leaman, K. D., and T. B. Sanford, 1975: Vertical energy propagation of inertial waves: A vector spectral analysis of velocity profiles. *J. Geophys. Res.*, **80**, 1975–1978.

Levine, M. D., C. A. Paulson, M. G. Briscoe, R. A. Weller, and H. Peters, 1983: Internal waves in JASIN. *Phil. Trans. Roy. Soc. London, Ser. A*, **308**, 389–405.

Levine, M. D., C. A. Paulson, and J. H. Morison, 1985: Internal waves in the Arctic Ocean: Comparison with lower-latitude observations. *J. Phys. Oceanogr.*, **15**, 800–809.

McComas, C. H., 1977: Equilibrium mechanisms within the oceanic internal wave field. *J. Phys. Oceanogr.*, **7**, 836–845.

Müller, P., D. J. Olbers, and J. Willebrand, 1978: The IWEX spectrum. *J. Geophys. Res.*, **83**, 479–500.

Müller, P., G. Holloway, F. Henyey, and N. Pomphrey, 1986: Nonlinear interactions among internal gravity waves. *Rev. Geophys.*, **24**, 493–536.

Padman, L., and T. M. Dillon, 1991: Turbulent mixing near the Yermak plateau during the Coordinated Eastern Arctic Experiment. *Geophys. Res.*, **96**, 4769–4782.

Pollard, R. T., and R. C. Millard, 1970: Comparison between observed and simulated wind-generated inertial oscillations. *Deep-Sea Res.*, **17**, 813–821.

Price, J. F., 1983: Internal wave wake of a moving storm. Part I: Scales, energy budget and observations. *J. Phys. Oceanogr.*, **13**, 949–965.

Thomson, R. E., 1983: A comparison between computed and measured oceanic winds near the British Columbia coast. *J. Geophys. Res.*, **88**, 2675–2683.

Watson, K. M., 1985: Interaction between internal waves and mesoscale flow. *J. Phys. Oceanogr.*, **15**, 1296–1311.

Webster, F., 1968: Observations of inertial-period motions in the deep sea. *Rev. Geophys.*, **6**, 473–490.

Wunsch, C., and S. Webb, 1979: The climatology of deep ocean internal waves. *J. Phys. Oceanogr.*, **9**, 235–243.